NMR chemical shifts of urea loaded copper benzoate. A joint solid-state NMR and DFT study.[†]

Zhipeng Ke, Lauren E. Jamieson, Daniel M. Dawson, Sharon E. Ashbrook,* Michael Bühl*

School of Chemistry, EaStCHEM and Centre of Magnetic Resonance
University of St Andrews
North Haugh, St Andrews, Fife, KY16 9ST, UK
E-mail: sema@st-andrews.ac.uk; buehl@st-andrews.ac.uk

Abstract

We report solid-state ^{13}C NMR spectra of urea-loaded copper benzoate, $Cu_2(C_6H_5CO_2)_4{\cdot}2$(urea), a simplified model for copper paddlewheel-based metal-organic frameworks (MOFs), along with first-principles density functional theory (DFT) computation of the paramagnetic NMR (pNMR) chemical shifts. Assuming a Boltzmann distribution between a diamagnetic open-shell singlet ground state (in a broken-symmetry Kohn-Sham DFT description) and an excited triplet state, the observed $\delta(^{13}C)$ values are reproduced reasonably well at the PBE0-⅓/IGLO-II//PBE0-D3/AE1 level. Using the proposed assignments of the signals, the mean absolute deviation between computed and observed ^{13}C chemical shifts is below 30 ppm over a range of more than 1100 ppm.

Introduction

Metal-organic frameworks (MOFs) are a well-known class of porous framework materials constructed from metal-based ions or clusters and organic linker molecules. The great interest in MOFs arises from the ease of modifying their structure and reactivity by changing the metal or linker species, allowing the properties of the MOF to be "tuned" for a specific application. Consequently, MOFs have been investigated for applications in fields such as sorption of harmful gases, catalysis and drug delivery.[1–3] Solid-state NMR spectroscopy is frequently used to study MOFs, particularly in cases where their local structure is dynamic or flexible.[4] In recent years, quantum-chemical calculations have been increasingly used alongside experimental solid-state NMR spectroscopy to aid spectral assignment and to provide detailed insight into even very complicated structures,[5,6] such that this approach is near ubiquitous for diamagnetic materials. However, for paramagnetic materials (including many popular MOFs), the calculation of NMR parameters is far from routine owing to the complicated electronic structure, which must often be handled on a case-by-case basis. This is unfortunate, as the NMR spectra of paramagnetic MOFs are often also complicated by a combination of paramagnetic shifts and relaxation effects, which can make it challenging to observe all resonances, let alone assign them.[7–10] Dawson *et al.* have carried out detailed ^{13}C NMR spectroscopy of the Cu(II)-based MOFs, HKUST-1, STAM-1 and STAM-17 using very fast magic-angle spinning (MAS),[9,11] and have shown that the copper "paddlewheel" dimer inorganic units lead to shifts ranging from *ca.* –100 to 850 ppm and, by using very costly and labour-intensive selective ^{13}C isotopic labelling, showed that the most shifted and broadened resonances (*i.e.*, those influenced most by paramagnetic effects) could not be assigned intuitively to the C species closest to the Cu centres.[9]

Despite the considerable theoretical challenge, pNMR calculations based on density functional theory (DFT) have already evolved to a stage where they can be useful both for locating and assigning signals in the experimental spectra, and for obtaining insights into the local structure.[12–14] So far,

[†] Dedicated to Prof. Walter Thiel on the occasion of his 70th birthday

many formalisms have been proposed to calculate pNMR chemical shifts for doublets[15] or for systems with arbitrary multiplicity.[16–19] In previous work[20] we have used the approach by Hrobárik and Kaupp [16] to compute the pNMR shifts of mononuclear Cu(II) phenolic oxime complexes, successfully reproducing the observed chemical shifts and their temperature dependence, as well as more subtle substituent effects.[12]

However, calculation of the complicated electronic structure of Cu(II) paddlewheel dimers is not straightforward as, although there is formally just one unpaired electron per Cu(II) centre, studies of the magnetic properties of these materials show that these electrons ferromagnetically couple to give an overall open-shell singlet ground state.[21] The antiferromagnetic coupling is weak, and thermal population of the triplet state should be readily possible at ambient temperatures. Magnetic measurements on STAM-1 indicate that, in an infinitely connected framework material, longer-range spin-spin interactions may also be present.[22,23] Therefore, in the present work, we have chosen to use a copper benzoate complex as a simplified model of the local structure of a copper paddlewheel MOF.

Copper benzoates of general formula $Cu_2(C_6H_5CO_2)_4 \cdot 2L$, where L is an axial ligand, are well known in the literature, having been extensively studied for their fungicidal and insecticidal activity, and have been prepared with a variety of axial ligands.[24,25] For the present work, we apply the computational approach described above to the ^{13}C NMR spectrum of the urea-loaded copper benzoate, $Cu_2(C_6H_5CO_2)_4 \cdot 2(urea)$, modelling the isotropic shifts through a thermal equilibrium between an antiferromagnetically coupled singlet ground state (devoid of pNMR shifts) and a ferromagnetically coupled paramagnetic excited state. This system poses a much more stringent test of the underlying methodology than the molecules and materials studied so far, because the observed chemical shifts are not only determined by the pNMR shifts of the actual paramagnetic species itself, [12–14,16,20,26] but also by the extent of its population in an equilibrium.[‡] Here, we validate the assumption of such an equilibrium through a Boltzmann distribution to calculate the isotropic pNMR shifts of $Cu_2(C_6H_5CO_2)_4 \cdot 2(urea)$.

Computational background

In a paramagnetic system the total chemical shift arises from the orbital shift (analogous to the chemical shift in diamagnetic systems), the Fermi contact shift (the interaction between the nuclear magnetic moment and the spin density at the position of the nucleus) and the pseudocontact shift (a long-range dipolar interaction between the induced magnetic moment at the radical site, and the nuclear magnetic moment).[15] The formalism (**Equation 1**) from Hrobárik and Kaupp[16] is applied to compute the paramagnetic shielding tensor σ. The isotropic value σ_{iso} is the trace of the shielding tensor.

$$\sigma_{iso} = \sigma_{iso(orb)} - S(S+1)\beta_e/(3kTg_N\beta_N)[g_e \cdot A_{FC} + g_e \cdot A_{PC} + \Delta g_{iso} \cdot A_{FC} + Tr(\Delta g_{aniso} \cdot A_{dip})/3] ,$$

Equation 1

where $\sigma_{iso(orb)}$ is the isotropic orbital shielding, S is the effective spin, β_e and β_N are the Bohr magneton and nuclear magneton, respectively, T is the absolute temperature, g_e and g_N are the free-electron and nuclear g values, respectively, A_{FC} and A_{dip} are the usual isotropic Fermi contact and anisotropic traceless spin-dipolar contributions to the A tensor, respectively, A_{PC} is the isotropic pseudocontact term arising from spin-orbit corrections to the A tensor, and Δg_{iso} and Δg_{aniso} are the isotropic and

[‡] For a previous case where observed chemical shifts have been interpreted in terms of thermal population of an excited paramagnetic state, see e.g.:[27].

anisotropic parts of the g tensor, respectively (in the usual representation of the g tensor in the form g = $g_e + \Delta g_{iso} \cdot 1 + \Delta g_{iso}$). Tr represents the trace of the matrix.

The calculated chemical shifts (δ) are quoted relative to a reference (typically tetramethylsilane (TMS), for ^{1}H and ^{13}C) using the equation below:

$$\delta \approx \sigma_{iso(orb)}(TMS) - \sigma_{iso}, \quad \textbf{Equation 2}$$

where the isotropic orbital shielding of the reference compound is computed using the same methodology.

The copper paddlewheel dimer contains two unpaired electrons, mostly located on the two copper atoms. The two copper atoms are connected by four bridging carboxylate groups, resulting in an antiferromagnetic coupling of the two spins,[28,29] affording a singlet ground state. The ferromagnetically coupled triplet excited state is slightly higher in energy (see below). As the overall spin is zero for the singlet ground state, there would be no pNMR shifts for this state (see **Equation 1**). It can therefore be assumed that the pNMR shifts in this system arise from the thermal equilibrium between the triplet and the singlet ground state. This equilibrium is evaluated through a Boltzmann distribution, which links the probability of finding each spin state with the energy gap between spin states and temperature:

$$x_{triplet} = N_{triplet}/N_{total} = g_{triplet} \exp(-\Delta E_{ST}/RT)/ [1+ g_{triplet} \exp(-\Delta E_{ST}/RT)] , \quad \textbf{Equation 3}$$

where x is the mole fraction, g is the degeneracy (= 3 for the triplet), ΔE_{ST} is the singlet-triplet energy gap, R is the gas constant and T is the absolute temperature. Consequently, the pNMR shielding can be calculated as,

$$\sigma_{total} = x_{singlet}\, \sigma_{singlet} + x_{triplet}\, \sigma_{triplet} \quad \textbf{Equation 4}$$

for calculating the pNMR chemical shifts, where $\sigma_{singlet}$ and $\sigma_{triplet}$ are the isotropic shieldings of the respective states evaluated from **Equation 1**, and $x_{singlet} = 1 - x_{triplet}$. ΔE_{ST} is taken as the exchange coupling constant J_{12} in the spin-coupling Hamiltonian $\hat{H}_s$ for two spin state operators $\hat{S}_1$ and $\hat{S}_2$[30]:

$$\hat{H}_s = -2J_{12}(\hat{S}_1\hat{S}_2) \quad \textbf{Equation 5}$$

See Experimental section at the end for further computational details.

Results and discussion

Copper benzoate can be co-crystallised with a variety of axial ligands, L. Complexes with urea are of interest in their own right, as this substrate can be used for many medical treatments.[31,32] A urea-loaded sample was prepared according to the method of Leban *et al.*, who have also characterised the structure using single-crystal X-ray diffraction.[19] **Figure 1a** shows the crystal structure of $Cu_2(C_6H_5CO_2)_4.2$(urea) and **Figure 1b** shows the structure of a single dimer complex within this material. The ^{13}C MAS NMR spectrum of $Cu_2(C_6H_5CO_2)_4.2$(urea) is shown in **Figure 1c**. Resonances are observed at 215, 178, 172, 164, 148, 131 and –47 ppm. Upon an offset of the transmitter frequency from 73 to 850 ppm and carrying out extensive signal averaging (see later Experimental section for details), a broad resonance was observed at ~1097 ppm (inset, **Figure 1c**).

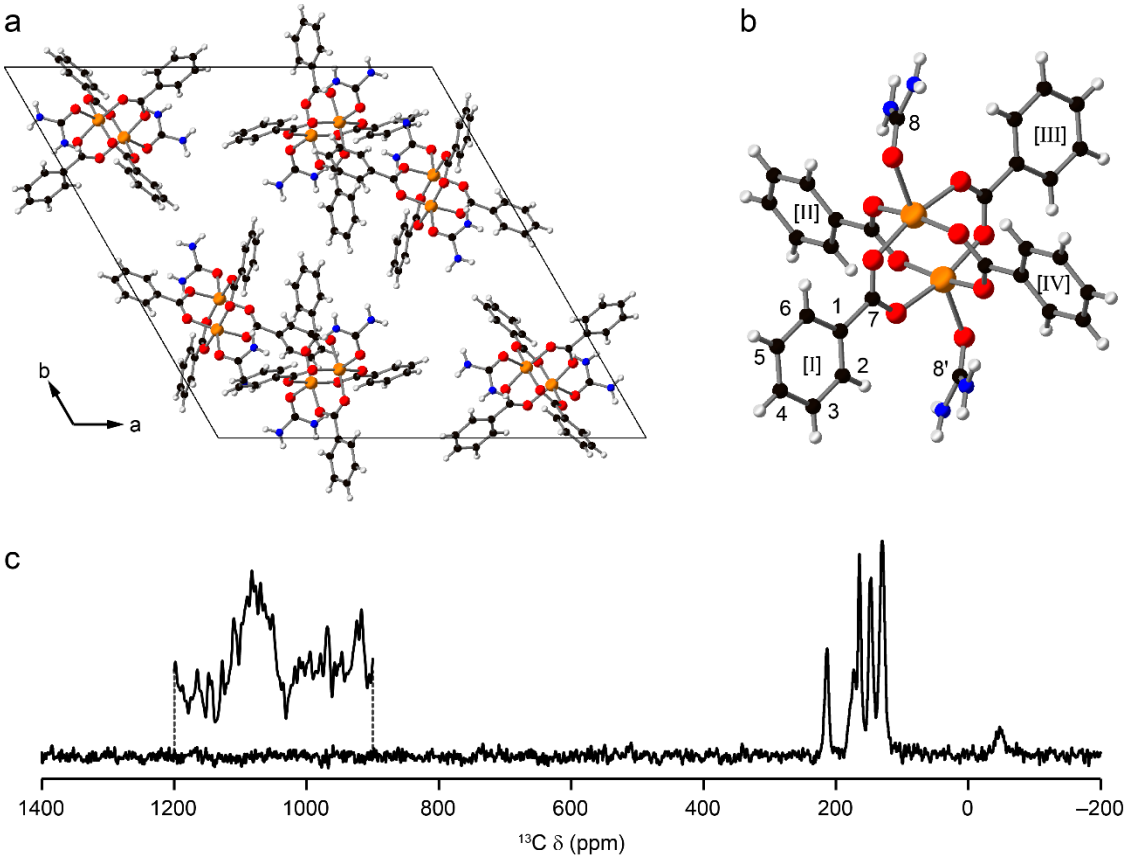

Figure 1. (a) The unit cell of $Cu_2(C_6H_5CO_2)_4$·2(urea) and (b) molecular structure (from reference [24]). Atoms are coloured with orange = Cu, red = O, blue = N, black = C, light grey = H. (c) ^{13}C (14.1 T, 60 kHz MAS) NMR spectrum of $Cu_2(C_6H_5CO_2)_4$.2(urea), recorded without temperature regulation (accounting for frictional heating, T ≈ 348 K), with the inset showing the broad resonance at *ca*. 1097 ppm, observed in a separate experiment with the transmitter offset at 850 ppm and with extensive signal averaging (see Experimental section).

The range of the observed shifts is quite similar to that observed for the copper paddlewheel-based MOFs HKUST-1, STAM-1 and STAM-17,[8,9,11,33] which exhibit very broad resonances at *ca.* 850 ppm, broad resonances at *ca.* –50 ppm and a series of sharper resonances between *ca*. 300 and 0 ppm, suggesting that this single-dimer complex is a good model compound for these materials. The crystal structure (**Figures 1a** and **1b**) shows two copper atoms surrounded by four equatorial benzoate ligands and two axial urea (guest) molecules. The two copper atoms are within bonding distance, 2.63 Å, comparable to the interatomic distance in bulk Cu metal, 2.64(8) Å.[34] At the PBE0-D3 level of theory, the optimised Cu-Cu distance in the $Cu_2(C_6H_5CO_2)_4$·2(urea) minimum is 2.62 Å, very close to the observed distance in the solid. As shown in **Figure 1a**, the individual paddlewheel dimers in the crystal are remote from each other (the shortest intermolecular Cu···Cu distance is 7.14 Å), and magnetic communication between them is expected to be weak. As previously demonstrated for mononuclear Cu(II) oximate complexes,[12,20] a single complex can, therefore, be used in the computational modelling without significantly affecting the calculated shifts.

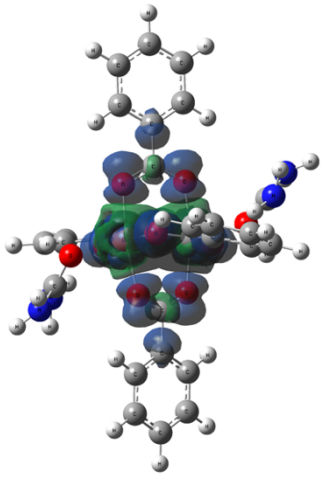

Figure 2. Spin density of $Cu_2(C_6H_5CO_2)_4{\cdot}2$(urea) in its triplet state (PBE0-⅓/IGLO-II//PBE0-D3/AE1 level, isodensity value for the surface at $\rho = 0.0004$ a.u.).

As expected for Cu(II) carboxylate paddlewheel dimers, antiferromagnetic coupling is computed for $Cu_2(C_6H_5CO_2)_4{\cdot}2$(urea), *i.e.*, the singlet is computed to be more stable than the triplet by around 134 cm^{-1} (PBE0-⅓/IGLO-II level, spin Hamiltonian defined in **Equation 5**), in qualitative agreement with experimental estimates for related Cu(II) carboxylate dimers.[29,35] The optimised Cu-Cu distance decreases from 2.618 Å in the singlet to 2.616 Å in the triplet (PBE0-D3 level).

There is no pNMR shift for the singlet state (only the "diamagnetic" $\sigma_{iso(orb)}$ term remains in **Equation 1** if S = 0), leading to the hypothesis that pNMR shifts arise from thermal population of the triplet state. In the triplet state, the expected hyperfine coupling from the isotropic Fermi-contact term (A_{FC} in **Equation 1**) can be visualised through the spin density, which shows the distribution of unpaired electrons (see **Figure 2**). As expected, the unpaired electron density is mostly centred on the Cu atoms (Mulliken spin densities of around 0.74), but there is notable spin delocalisation onto the equatorial ligands through the Cu-O, O-C and C-C bonds. Among the carbon atoms, the benzoic *ipso* carbon C1 and the carboxylate carbon C7 in each of the four benzoate ligands (see numbering scheme in **Figure 1b**) carry the largest spin densities. These spin densities have opposite signs (*cf.* the different colours on these atoms in **Figure 2**). Assuming the isotropic A_{FC} term dominates the pNMR shifts, this spin distribution suggests that the experimental "extreme" shift values at 1079 ppm and –47 ppm originate from these carbon atoms. Using ^{13}C isotopic labelling experiments, Dawson *et al.*[9] were able to assign the corresponding peaks in the ^{13}C MAS NMR spectra of STAM-1 and HKUST-1, which both contain the copper paddlewheel dimer as a building block. In these MOFs, the benzoic *ipso* and carboxylate carbon atoms were assigned to the most deshielded (853 ppm) and most shielded resonances (–50 ppm), respectively. Based on these findings, it is reasonable to assign the shifts in $Cu_2(C_6H_5CO_2)_4.2$(urea) at 1079 ppm and –47 ppm to the analogous carbon species, which is fully consistent with the spin density in **Figure 2**.

In the solid, the molecules have an inversion centre at the midpoint of the two Cu atoms (*R*–3 space group). When the isolated molecules are optimised in C_i symmetry, they are not minima, but transition states with low imaginary frequencies for both the singlet and triplet state structures. Following the imaginary modes affords true minima, which have C_1 symmetry. However, these structures are quite similar to those in C_i, and their energies are within *ca.* 1 kJ mol^{-1} of each other (*e.g.*, for the triplet, the C_1 minimum is lower than the C_i transition state by only 0.7 kJ mol^{-1} at the PBE0-D3 + ZPE level, see **Tables S1** and **S2** in the **ESI**). We therefore calculate the shifts for the C_1 minima, but assume rapid averaging to an overall apparent C_i symmetry (very similar δ values are obtained when

the chemical shifts are computed for the C_i transition states, see **Table S3** in the **ESI**). In C_i symmetry, there are 15 non-equivalent carbon sites (including urea). Only 8 signals are resolved in the experimental ^{13}C NMR spectrum, suggesting that some signals may be coincidentally degenerate (or too closely spaced to be resolved) and/or that dynamic averaging takes place, *e.g.* through fast rotation of the phenyl rings or the urea ligands (*i.e.*, fast on the NMR timescale; note that the measurements were taken at a slightly elevated temperature, ~348 K, whereas the crystal structure was obtained at the lower temperature of 293 K). Rapid rotation of the urea ligands and all rings together can be excluded as this would lead to apparent D_{4h} symmetry, and just 6 signals in the NMR spectrum.

The computed ^{13}C NMR chemical shifts are given in **Table 1**. The first two entries show that neither the data for triplet or singlet states alone can rationalise the observed chemical shift range - the singlet state, devoid of pNMR contributions, only has resonances in the normal range associated with aromatic carbons (*i.e.*, between *ca*. 130 and 180 ppm), whereas the triplet state has resonances at the more shielded and deshielded extremes of the spectrum (*ca*. –400 to 1600 ppm) that significantly exceed the observed shifts (*ca*. –50 to 1100 ppm). Averaging singlet and triplet chemical shifts according to the proposed thermal equilibrium (**Equations 3** and **4**, using a DFT-computed energy gap ΔE_{ST}, see computational details) affords resonances that are in reasonably good agreement with the observed shift range (see column "total" in **Table 1**). The largest deviation is seen at the more shielded end of the range, where shifts around δ = –200 ppm are computed for the singlet-triplet equilibrium mixture, significantly overestimating the observed value of δ = –47 ppm.

Evidently the position of this equilibrium and, thus, the final pNMR results will depend noticeably on the singlet-triplet energy gap, which we use directly as calculated. To probe the sensitivity of the computed chemical shifts on this parameter, we have evaluated these for other selected values of ΔE_{ST} (see **Table S5** in the **ESI**). Changing this parameter by ±10% introduces only minor changes (up to ±19 ppm for the most deshielded resonance assigned to C1). Changing it to the mean value obtained experimentally for a large number of dinuclear copper carboxylate complexes, 296 cm^{-1}[29], causes the agreement with experiment to deteriorate (in particular for the most deshielded resonance, which then deviates by more than 250 ppm, see **Table S5**). As no experimental value is known for the urea adduct of our study, and because the energy gap can depend on the nature of the carboxylate and the guest molecule, we did not try to adjust the ΔE_{ST} value, but use it as calculated.

When ordering the chemical shifts of all C atoms by magnitude, it appears that they fall in groups of four (in C_1 symmetry, but in groups of two when averaged to C_i), or, for urea, a group of two (a single shift when averaged to C_i) with very similar values. Some larger spreads (on the order of 30 to 40 ppm) are computed for the individual signals at the shielded and deshielded extremities of the range but, here, the observed experimental resonances are very broad. For all signals in between, the computed spread of the individual resonances is much smaller, typically between 1 and 5 ppm. Such small separations are not resolved experimentally, as even the sharpest resonance is on the order of 5 ppm full width half height. For a tentative spectral assignment, we therefore assume static C_i structures with overlapping signals as indicated in **Table 1**. In essence, we assume both sets of *ortho* and *meta* resonances within each phenyl ring to be essentially equivalent (either through non-resolvable overlap of the signals or through rapid rotation of the Ph rings), but assume different, resolvable, signals for pairs of phenyl rings (in which case no rapid rotation of the urea guests could occur). The resulting assignment (compare "Average $\delta_{(total)}$" and "Expt $\delta_{(total)}$" in **Table 1**) leads to an overall satisfactory agreement between theory and experiment. The largest error is significant, more than 150 ppm for the carboxylate carbon atoms C7, but all other absolute deviations are 20 ppm or less, with an overall mean absolute error of 27.2 ppm. While this absolute error may appear large, it is less than 2.5% of the total observed shift range of ~1100 ppm, which is comparable to the errors one would expect for diamagnetic materials.[36] This is particularly impressive considering the challenging electronic structure of the material.

Table 1. Calculated ^{13}C chemical shifts $\delta_{(total)}$ [in ppm] for $Cu_2(C_6H_5CO_2)_4 \cdot 2(urea)$ using **Equations 1-4**, with ΔE_{ST} = 134.59 cm^{-1} (PBE0-⅓/IGLO-II//PBE0-D3/AE1), C_1 symmetry at 348 K[a]

Site	Calculated δ			Average $\delta_{(total)}$	Expt $\delta_{(total)}$	Absolute error $\lvert$Expt $\delta_{(total)}$ – Calc $\delta_{(total)}\rvert$
	Triplet	Singlet	Total			
C1I	1634.2	139.8	1084.7	1061.7	1079	17.3
C1II	1603.9	140.0	1065.6			
C1IV	1586.5	139.8	1054.6			
C1III	1566.7	139.3	1041.8			
C2II	229.3	137.8	195.6	194.5[b]	215	20.5
C6IV	228.7	137.8	195.3			
C6II	226.9	136.3	193.6			
C2IV	226.7	136.7	193.6			
C2I	218.0	136.0	187.9	185.4[b]	178	7.4
C6III	213.4	136.3	185.0			
C6I	211.9	138.1	184.8			
C2III	210.3	138.1	183.8			
C3I	197.5	132.5	173.6	168.2[b]	172	3.8
C5II	195.6	131.9	172.2			
C3II	193.5	133.0	171.3			
C5I	191.5	133.0	170.0			
C3IV	189.8	132.0	168.5	169.8[b]	164	5.8
C5IV	187.5	132.7	167.3			
C5III	185.4	132.5	166.0			
C3III	180.7	132.9	163.1			
C8	146.9	171.0	155.7	155.2	148	7.2
C8'	145.3	170.9	154.7			
C4III	134.0	137.7	135.4	132.3	131	1.3
C4IV	131.2	137.2	133.4			
C4II	126.5	137.3	130.5			
C4I	125.6	137.7	130.0			
C7II	–390.4	180.2	–180.6	–201.3	–47	154.3
C7IV	–430.1	180.7	–205.5			
C7I	–435.8	180.6	–209.1			
C7III	–436.9	180.8	–209.8			
Mean ansolute error						27.2

[a]See **Figure 1b** for the numbering scheme used. [b]Averaged according to C_i symmetry, *e.g.*, C3I, C5I, C3III and C5III are grouped, and C3II, C5II, C3IV and C5IV are grouped separately.

The quality of the resulting assignment is illustrated by the plot of the computed shifts against those observed experimentally, shown in **Figure 3**. The overestimated shielding of the resonance at negative shift notwithstanding, the degree of agreement between theory and experiment is pleasing. It is remarkable that this agreement is achieved using standard broken-symmetry DFT results (including the calculated singlet-triplet gap) without scaling or further tweaking of the exchange-correlation functional that had been validated for different (mononuclear) systems.[12,20] This finding lends strong support to our underlying assumption of an equilibrium between an open-shell singlet ground

state and a thermally populated excited triplet state, which is ultimately responsible for the observed pNMR chemical shifts. We note in passing that this degree of agreement is only achieved when the degeneracy factor for the triplet is included in the Boltzmann distribution (**Equation 3** - an illustration of its importance is given in **Figure S2** in the **ESI**). Although compared with experimental values (D = –0.335 cm^{-1}, E/D = 0.030) for the hydrated copper acetate analogue [37] the calculated D value (D = 23.364 cm^{-1}, E/D = 0.0288) may be notably overestimated, we note that the effect of zero-field splitting in the computed shieldings of the triplet is negligible (see **Table S4** in the **ESI**).

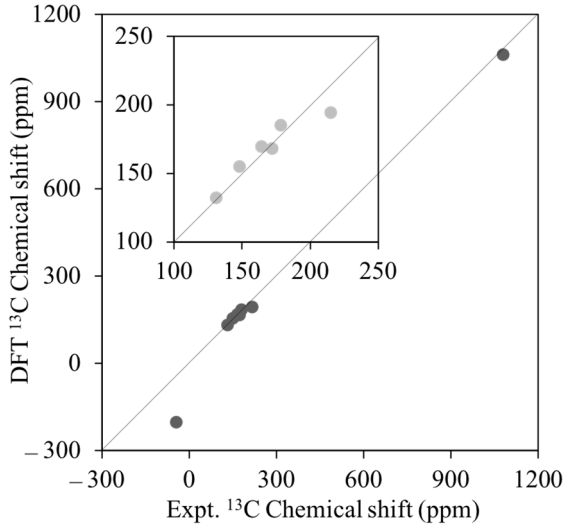

Figure 3. Plot of calculated (PBE0-⅓ level of DFT) against experimental (348 K) ^{13}C chemical shifts of $Cu_2(C_6H_5CO_2)_4 \cdot 2(urea)$ ($\delta_{(total)}$ data from **Table 1**). The inset with the light grey dots is an expansion of the aromatic region.

Further experimental support for the assignment presented here would require the acquisition of a more quantitative spectrum, along with multinuclear ^{1}H-^{13}C correlation experiments, which have previously been demonstrated to be effective for identifying protonated C species even in paramagnetic systems.[9,11,12,20,38] However, in this case, full assignment *via* this approach would still be very challenging as there is very little resolution of the ^{1}H resonances (see **Figure S3** in the **ESI**). Support for assignments could also come from chemical shift anisotropies which, in principle, could be measured at lower MAS rates. However, the more interesting, paramagnetically shifted NMR signals are very broad due to rapid relaxation and tend to become undetectable at lower spinning frequencies. For future reference, the computed full shielding tensors are reported in **Table S7** in the **ESI**.

Breakdown of the computed magnetic shielding constants of the triplet into the contributions arising from **Equation 1** confirms that the isotropic hyperfine coupling (in form of the $g_e \bullet A_{FC}$ and, to a lesser extent, the $\Delta g_{iso} \bullet A_{FC}$ terms) makes by far the largest contribution to the pNMR shifts. For example, for the most deshielded (C1) and shielded (C7) nuclei the $g_e \bullet A_{FC}$ term alone contributes $\Delta\delta \approx +1400$ ppm and $\Delta\delta \approx -530$ ppm, respectively (see **Table S6** in the **ESI**), to the total shifts of $\delta \approx +1600$ ppm and $\delta \approx -430$ ppm, respectively (see triplet entries in **Table 1**). It is thus entirely reasonable to interpret the pNMR shifts based on (isotropic) spin densities, as illustrated in **Figure 2**.

Conclusion

In summary, we have recorded the solid-state ^{13}C MAS NMR spectrum of $Cu_2(C_6H_5CO_2)_4 \cdot 2(urea)$, a model compound for MOFs containing the copper paddlewheel dimer structural motif, and have reproduced the chemical shifts computationally with a state-of-the-art DFT methodology. Observed $\delta(^{13}C)$ values outside the "normal" ^{13}C chemical shift range, in particular at δ = 1079 ppm, clearly indicate the presence of paramagnetic centres. Because the individual paddlewheel dimers that form the crystal have a singlet ground state (antiferromagnetic coupling of the two spins on either Cu), the hypothesis for the source of the observed pNMR shifts is the thermal population of an excited triplet state (ferromagnetic coupling of the two spins). This hypothesis is fully borne out by our calculations, which are based on a Boltzmann distribution of singlet and triplet states at the temperature of the experiment and a corresponding averaging of the computed chemical shifts for each state. Using a methodology that had been validated for mononuclear Cu(II) species, which involves exchange-correlation functionals with a high fraction of Hartree-Fock exchange (PBE0-⅓ in this case) to compute the pNMR shifts of the triplet, the observed chemical shift pattern is reproduced very well qualitatively, and even satisfactorily in a quantitative sense, with a mean absolute deviation between computed and observed $\delta(^{13}C)$ values on the order of 30 ppm over a range of more than 1100 ppm. This degree of agreement is achieved with standard broken-symmetry DFT results (including the calculated singlet-triplet gap) without scaling or further tweaking of the exchange-correlation functional. To be able to describe a system with such a complicated electronic structure computationally is, arguably, a major advance in the non-empirical calculation of pNMR shifts.

Although the peaks in the region of the spectrum where aromatic species are typically found (between 148 and 178 ppm) are hard to assign, the “extreme” shifts (at –47, 215 and 1079 ppm) match fairly well and can be assigned with confidence. This result is very promising for the envisaged modelling of more elaborate MOF models, where communication between the paddlewheel dimers through aromatic linkers is possible.

Hopefully these results will allow the construction of suitable models to predict the NMR properties of MOFs that contain copper paddlewheel dimer building blocks. Ultimately, the goal is to combine experiment and computation into a structural tool for paramagnetic materials, hopefully as powerful as it is already for diamagnetic ones.

Experimental and Computational details

$Cu_2(C_6H_5CO_2)_4.2(urea)$ was synthesised according to the method of Leban *et al.*[24]: $CuSO_4.5H_2O$ (0.50 g, 2.0 mmol) in methanol was acidified with a few drops of 20% H_2SO_4 and mixed with a solution of sodium benzoate (0.58 g, 4.0 mmol) and urea (0.37 g, 6.2 mmol) in methanol. The mixture was left undisturbed at room temperature until blue crystals of product formed. The product was then isolated by suction filtration and washed with methanol.

Solid-state NMR spectra were recorded using a Bruker Avance III spectrometer equipped with a 14.1 T wide-bore superconducting magnet (Larmor frequencies of 600.1 and 150.9 MHz for ^{1}H and ^{13}C, respectively). The large crystals of $Cu_2(C_6H_5CO_2)_4.2(urea)$ were finely ground and packed into a zirconia MAS rotor of outer diameter 1.3 mm, which was then rotated at the magic angle at 60 kHz under ambient conditions (estimated temperature of 348 K, including frictional heating effects). Spectra were recorded using a spin-echo experiment, with a rotor-synchronised echo delay of 16.7 μs. The spectrum shown in **Figure 1c** was recorded by averaging 51,200 transients with a recycle interval of 100 ms, and the spectrum in the inset was recorded with a transmitter offset of 850 ppm and signal averaging of 525,056 transients with a recycle interval of 100 ms. The ^{1}H MAS NMR spectrum shown in the **ESI** was recorded with a rotor-synchronised spin-echo experiment, with signal

averaging of 512 transients with a recycle interval of 100 ms. Shifts are reported in ppm relative to $(CH_3)_4Si$ using L-alanine as a secondary solid reference (^{13}C $\delta(\mathbf{C}H_3)$ = 20.5 ppm, ^{1}H $\delta(N\mathbf{H}_3)$ = 8.5 ppm).

The DFT computational methodologies used in this paper are similar to the method introduced by Bühl *et al.* and Dawson *et al.* [12,20] Structural optimisation was performed using Gaussian 09[39] at the PBE0-D3 level.[40–44] An augmented Wachters basis set [45,46] was used for Cu (8s7p4d) with full contraction scheme 62111111/3311111/3111. The 6-31G** basis set was used on the urea molecules attached to the paramagnetic centres of the paddlewheel dimer, while 6-31G* was used for the remaining atoms (this combination of basis sets is labelled AE1). The structure optimisation was carried out separately for each spin state using unrestricted Kohn-Sham wavefunctions with a broken-symmetry solution for the open-shell singlet (*e.g.*, expectation values of the $\hat{S}^2$ operator of 0.995 and 2.004 for the singlet and triplet in the C_1 minimum, respectively). The character of each stationary point was verified by computation of the harmonic vibrational frequencies, which were all real for the C_1 minima and showed one imaginary frequency for the C_i structures. The frequencies were also used to obtain thermodynamic corrections to relative enthalpies and free energies. NMR parameters were computed for these PBE0-D3 optimised structures at the PBE0-⅓ level,[47] employing a 9s7p4d (621111111/3311111/3111) basis set on Cu, which was constructed specifically for accurate hyperfine coupling constant calculations,[48] and IGLO-basis II [49] on the ligands (this combination of basis sets is labelled IGLO-II). Orbital shieldings $\sigma_{iso(orb)}$ were computed using the GIAO (gauge-including atomic orbitals) implementation in Gaussian 09 for both singlet and triplet states in their respective PBE0-D3/AE1 optimised structures. The computed isotropic orbital shielding of the reference compound is 189.0 ppm for ^{13}C in TMS at the same level of theory. The hyperfine coupling and g tensors were computed for the triplet state at the PBE0-⅓/IGLO-II level using the ORCA program.[50] This level has performed very well in pNMR computations of metallocenes [16] and phenolic Cu(II) oximes.[12,20] ΔE_{ST} was evaluated at PBE0-⅓/IGLO-II level using the broken-symmetry approach of Noodleman.[21,51,52] The final computed chemical shifts are moderately sensitive toward this parameter, but only at the extreme shielded and deshielded ends (see **Table S5** in the **ESI**). The ZFS parameters have been calculated using the coupled-perturbed method by Neese[53] at the PBE/IGLO-II level (for technical reasons only a non-hybrid functional could be used here).

Acknowledgments.

We thank EaStCHEM and the School of Chemistry for support. Computations were carried out on a local Opteron PC cluster maintained by Dr. H. Früchtl. This work was supported by the EPSRC through the Collaborative Computational Project on NMR Crystallography (CCP-NC), via EP/M022501/1. SEA would also like to thank the Royal Society and Wolfson Foundation for a merit award. ZK gratefully appreciates a scholarship from the China Scholarship Council (CSC). We also thank Prof. A. M. Z. Slawin and Hanna Boström for analytical support. For research data supporting this publication see DOI: XXXX.[54]

References

[1] K. Sumida, D.L. Rogow, J.A. Mason, T.M. McDonald, E.D. Bloch, Z.R. Herm, T.-H. Bae, J.R. Long, Carbon Dioxide Capture in Metal–Organic Frameworks, Chem. Rev. 112 (2012) 724–781. doi:10.1021/cr2003272.

[2] M.P. Suh, H.J. Park, T.K. Prasad, D.-W. Lim, Hydrogen storage in metal-organic frameworks, Chem. Rev. 112 (2011) 782–835. doi:10.1002/adma.200902096.

[3] A.C. McKinlay, R.E. Morris, P. Horcajada, G. Férey, R. Gref, P. Couvreur, C. Serre, BioMOFs: Metal-Organic Frameworks for Biological and Medical Applications, Angew. Chemie Int. Ed. 49 (2010) 6260–6266. doi:10.1002/anie.201000048.

[4] S.E. Ashbrook, D.M. Dawson, V.R. Seymour, Recent developments in solid-state NMR spectroscopy of crystalline microporous materials, Phys. Chem. Chem. Phys. 16 (2014) 8223–8242. doi:10.1039/C4CP00578C.

[5] T. Charpentier, The PAW/GIPAW approach for computing NMR parameters: A new dimension added to NMR study of solids, Solid State Nucl. Magn. Reson. 40 (2011) 1–20. doi:10.1016/j.ssnmr.2011.04.006.

[6] S.E. Ashbrook, D. McKay, Combining solid-state NMR spectroscopy with first-principles calculations – a guide to NMR crystallography, Chem. Commun. 52 (2016) 7186–7204. doi:10.1039/C6CC02542K.

[7] S.E. Ashbrook, D.M. Dawson, J.M. Griffin, Solid-State NuclearMagnetic Resonance Spectroscopy, in: D.W. Bruce, D. O'Hare, R.I. Walton (Eds.), Local Struct. Characterisation Inorg. Mater. Ser., 1st ed., WILEY, West Sussex, 2013: pp. 1–88.

[8] F. Gul-E-Noor, B. Jee, A. Pöppl, M. Hartmann, D. Himsl, M. Bertmer, Effects of varying water adsorption on a Cu3(BTC)2metal-organic framework (MOF) as studied by1H and13C solid-state NMR spectroscopy, Phys. Chem. Chem. Phys. 13 (2011) 7783–7788. doi:10.1039/c0cp02848g.

[9] D.M. Dawson, L.E. Jamieson, M.I.H. Mohideen, A.C. McKinlay, I.A. Smellie, R. Cadou, N.S. Keddie, R.E. Morris, S.E. Ashbrook, High-resolution solid-state 13C NMR spectroscopy of the paramagnetic metal–organic frameworks, STAM-1 and HKUST-1, Phys. Chem. Chem. Phys. 15 (2013) 919–929. doi:10.1039/C2CP43445H.

[10] G. de Combarieu, M. Morcrette, F. Millange, N. Guillou, J. Cabana, C.P. Grey, I. Margiolaki, G. Férey, J.-M. Tarascon, Influence of the Benzoquinone Sorption on the Structure and Electrochemical Performance of the MIL-53(Fe) Hybrid Porous Material in a Lithium-Ion Battery, Chem. Mater. 21 (2009) 1602–1611. doi:10.1021/cm8032324.

[11] D.M. Dawson, C.E.F. Sansome, L.N. McHugh, L. McCormick, M.J. McPherson, R.E. Morris, S.E. Ashbrook, 13C pNMR of "Crumple Zone" Cu(II) Isophthalate Metal-Organic Frameworks, Submitted to Solid State Nucl. Magn. Reson. (this issue).

[12] D.M. Dawson, Z. Ke, F.M. Mack, R.A. Doyle, G.P.M. Bignami, I.A. Smellie, M. Bühl, S.E. Ashbrook, Calculation and experimental measurement of paramagnetic NMR parameters of phenolic oximate Cu(ii) complexes, Chem. Commun. 53 (2017) 10512–10515. doi:10.1039/C7CC05098D.

[13] T. Wittmann, A. Mondal, C.B.L. Tschense, J.J. Wittmann, O. Klimm, R. Siegel, B. Corzilius, B. Weber, M. Kaupp, J. Senker, Probing Interactions of N-Donor Molecules with Open Metal Sites within Paramagnetic Cr-MIL-101: A Solid-State NMR Spectroscopic and Density Functional Theory Study, J. Am. Chem. Soc. 140 (2018) 2135–2144. doi:10.1021/jacs.7b10148.

[14] X. Xu, S.C.F. Au-Yeung, A DFT and 59 Co Solid-State NMR Study of the Chemical Shielding Property and Electronic Interaction in the Metalloporphyrin System, J. Am. Chem. Soc. 122 (2000) 6468–6475. doi:10.1021/ja9911723.

[15] S. Moon, S. Patchkovskii, First-Principles Calculation of NMR and EPR Parameters, Wiley-VCH Verlag GmbH & Co. KGaA, Weinheim, FRG, 2004. doi:10.1002/3527601678.

[16] P. Hrobárik, R. Reviakine, A. V. Arbuznikov, O.L. Malkina, V.G. Malkin, F.H. Köhler, M. Kaupp, Density functional calculations of NMR shielding tensors for paramagnetic systems

with arbitrary spin multiplicity: Validation on 3d metallocenes, J. Chem. Phys. 126 (2007) 024107. doi:10.1063/1.2423003.

[17] W. Van den Heuvel, A. Soncini, NMR chemical shift as analytical derivative of the Helmholtz free energy, J. Chem. Phys. 138 (2013) 054113. doi:10.1063/1.4789398.

[18] B. Martin, J. Autschbach, Temperature dependence of contact and dipolar NMR chemical shifts in paramagnetic molecules, J. Chem. Phys. 142 (2015) 054108. doi:10.1063/1.4906318.

[19] T.O. Pennanen, J. Vaara, Nuclear Magnetic Resonance Chemical Shift in an Arbitrary Electronic Spin State, Phys. Rev. Lett. 100 (2008) 133002. doi:10.1103/PhysRevLett.100.133002.

[20] M. Bühl, S.E. Ashbrook, D.M. Dawson, R.A. Doyle, P. Hrobárik, M. Kaupp, I.A. Smellie, Paramagnetic NMR of Phenolic Oxime Copper Complexes: A Joint Experimental and Density Functional Study, Chem. Eur. J. 22 (2016) 15328–15339. doi:10.1002/chem.201602567.

[21] F. Neese, Prediction of molecular properties and molecular spectroscopy with density functional theory: From fundamental theory to exchange-coupling, Coord. Chem. Rev. 253 (2009) 526–563. doi:10.1016/j.ccr.2008.05.014.

[22] M.I.H. Mohideen, Novel Metal Organic Frameworks: Synthesis , Characterization and Functions, University of St. Andrews, 2011.

[23] H. El Mkami, M.I.H. Mohideen, C. Pal, A. McKinlay, O. Scheimann, R.E. Morris, EPR and magnetic studies of a novel copper metal organic framework (STAM-I), Chem. Phys. Lett. 544 (2012) 17–21. doi:10.1016/j.cplett.2012.06.012.

[24] I. Leban, N. Grgurevic, J. Sieler, P. Segedin, Tetrakis(μ-benzoato- O : O ')bis(urea)-1κ O ,2κ O -dicopper(II), Acta Crystallogr. Sect. C Cryst. Struct. Commun. 53 (1997) 854–856. doi:10.1107/S0108270197003387.

[25] M. Melník, M. Kabešová, M. Koman, Ľ. Macášková, J. Garaj, C.E. Holloway, A. Valent, COPPER(II) COORDINATION COMPOUNDS: CLASSIFICATION AND ANALYSIS OF CRYSTALLOGRAPHIC AND STRUCTURAL DATA III. DIMERIC COMPOUNDS, J. Coord. Chem. 45 (1998) 147–359. doi:10.1080/00958979808027144.

[26] J. Lee, I.D. Seymour, A.J. Pell, S.E. Dutton, C.P. Grey, A systematic study of 25 Mg NMR in paramagnetic transition metal oxides: applications to Mg-ion battery materials, Phys. Chem. Chem. Phys. 19 (2017) 613–625. doi:10.1039/C6CP06338A.

[27] B. Le Guennic, T. Floyd, B.R. Galan, J. Autschbach, J.B. Keister, Paramagnetic Effects on the NMR Spectra of “Diamagnetic” Ruthenium(bis-phosphine)(bis-semiquinone) Complexes, Inorg. Chem. 48 (2009) 5504–5511. doi:10.1021/ic802302v.

[28] K.A.H. Alzahrani, R.J. Deeth, Density functional calculations reveal a flexible version of the copper paddlewheel unit: implications for metal organic frameworks, Dalt. Trans. 45 (2016) 11944–11948. doi:10.1039/C6DT01474G.

[29] R.W. Jotham, S.F.A. Kettle, J.A. Marks, Antiferromagnetism in transition-metal complexes. Part IV. Lowlying excited states of binuclear copper(II) carboxylate complexes, J. Chem. Soc. Dalt. Trans. (1972) 428. doi:10.1039/dt9720000428.

[30] A.P. Ginsberg, Magnetic exchange in transition metal complexes. 12. Calculation of cluster exchange coupling constants with the X.alpha.-scattered wave method, J. Am. Chem. Soc. 102 (1980) 111–117. doi:10.1021/ja00521a020.

[31] G. Decaux, C. Andres, F. Gankam Kengne, A. Soupart, Treatment of euvolemic hyponatremia in the intensive care unit by urea, Crit. Care. 14 (2010) R184. doi:10.1186/cc9292.

[32] H. CRAWFORD, THE USE OF UREA AS A DIURETIC IN ADVANCED HEART

FAILURE, Arch. Intern. Med. 36 (1925) 530. doi:10.1001/archinte.1925.00120160088004.

[33] L.N. McHugh, M.J. McPherson, L.J. McCormick, S.A. Morris, P.S. Wheatley, S.J. Teat, D. McKay, D.M. Dawson, C.E.F. Sansome, S.E. Ashbrook, C.A. Stone, M.W. Smith, R.E. Morris, Hydrolytic stability in hemilabile metal–organic frameworks, Nat. Chem. (2018). doi:10.1038/s41557-018-0104-x.

[34] B. Cordero, V. Gómez, A.E. Platero-Prats, M. Revés, J. Echeverría, E. Cremades, F. Barragán, S. Alvarez, Covalent radii revisited, Dalt. Trans. (2008) 2832. doi:10.1039/b801115j.

[35] S. Yamada, H. Nishikawa, S. Miki, Spectrochemical Study of Microscopic Crystals. XXIV. The Structure and Light Absorption of Copper(II) Complexes of Benzoic and Substituted Benzoic Acids, Bull. Chem. Soc. Jpn. 37 (1963) 576–581. https://doi.org/10.1246/bcsj.37.576.

[36] C. Bonhomme, C. Gervais, F. Babonneau, C. Coelho, F. Pourpoint, T. Azaïs, S.E. Ashbrook, J.M. Griffin, J.R. Yates, F. Mauri, C.J. Pickard, First-Principles Calculation of NMR Parameters Using the Gauge Including Projector Augmented Wave Method: A Chemist's Point of View, Chem. Rev. 112 (2012) 5733–5779. doi:10.1021/cr300108a.

[37] A. Ozarowski, The Zero-Field-Splitting Parameter D in Binuclear Copper(II) Carboxylates Is Negative, Inorg. Chem. 47 (2008) 9760–9762. doi:10.1021/ic801560e.

[38] A.J. Pell, G. Pintacuda, C.P. Grey, Paramagnetic NMR in solution and the solid state, Prog. Nucl. Magn. Reson. Spectrosc. 111 (2018) 1–271. doi:10.1016/j.pnmrs.2018.05.001.

[39] M.J. Frisch, G.W. Trucks, H.B. Schlegel, G.E. Scuseria, M.A. Robb, J.R. Cheeseman, G. Scalmani, V. Barone, B. Mennucci, G.A. Petersson, H. Nakatsuji, M. Caricato, X. Li, H.P. Hratchian, A.F. Izmaylov, J. Bloino, G. Zheng, J.L. Sonnenberg, M. Hada, M. Ehara, K. Toyota, R. Fukuda, J. Hasegawa, M. Ishida, T. Nakajima, Y. Honda, O. Kitao, H. Nakai, T. Vreven, J.A. Montgomery, J.E. Peralta, F. Ogliaro, M. Bearpark, J.J. Heyd, E. Brothers, K.N. Kudin, V.N. Staroverov, T. Keith, R. Kobayashi, J. Normand, K. Raghavachari, A. Rendell, J.C. Burant, S.S. Iyengar, J. Tomasi, M. Cossi, N. Rega, J.M. Millam, M. Klene, J.E. Knox, J.B. Cross, V. Bakken, C. Adamo, J. Jaramillo, R. Gomperts, R.E. Stratmann, O. Yazyev, A.J. Austin, R. Cammi, C. Pomelli, J.W. Ochterski, R.L. Martin, K. Morokuma, V.G. Zakrzewski, G.A. Voth, P. Salvador, J.J. Dannenberg, S. Dapprich, A.D. Daniels, O. Farkas, J.B. Foresman, J. V. Ortiz, J. Cioslowski, D.J. Fox, J.A. Montgomery Jr., J.E. Peralta, F. Ogliaro, M. Bearpark, J.J. Heyd, E. Brothers, K.N. Kudin, V.N. Staroverov, R. Kobayashi, J. Normand, K. Raghavachari, A. Rendell, J.C. Burant, S.S. Iyengar, J. Tomasi, M. Cossi, N. Rega, J.M. Millam, M. Klene, J.E. Knox, J.B. Cross, V. Bakken, C. Adamo, J. Jaramillo, R. Gomperts, R.E. Stratmann, O. Yazyev, A.J. Austin, R. Cammi, C. Pomelli, J.W. Ochterski, R.L. Martin, K. Morokuma, V.G. Zakrzewski, G.A. Voth, P. Salvador, J.J. Dannenberg, S. Dapprich, A.D. Daniels, Ö. Farkas, J.B. Foresman, J. V. Ortiz, J. Cioslowski, D.J. Fox, Gaussian 09, Revision D.01, Gaussian Inc. (2013). doi:10.1159/000348293.

[40] J.P. Perdew, Y. Wang, Accurate and simple analytic representation of the electron-gas correlation energy, Phys. Rev. B. 45 (1992) 13244–13249. doi:10.1103/PhysRevB.45.13244.

[41] J.P. Perdew, M. Ernzerhof, K. Burke, Rationale for mixing exact exchange with density functional approximations, J. Chem. Phys. 105 (1996) 9982–9985. doi:10.1063/1.472933.

[42] S. Grimme, J. Antony, S. Ehrlich, H. Krieg, A consistent and accurate ab initio parametrization of density functional dispersion correction (DFT-D) for the 94 elements H-Pu, J. Chem. Phys. 132 (2010) 154104. doi:10.1063/1.3382344.

[43] A.D. Becke, E.R. Johnson, A density-functional model of the dispersion interaction, J. Chem. Phys. 123 (2005) 154101. doi:10.1063/1.2065267.

[44] E.R. Johnson, A.D. Becke, A post-Hartree-Fock model of intermolecular interactions: Inclusion of higher-order corrections, J. Chem. Phys. 124 (2006) 174104.

doi:10.1063/1.2190220.

[45] A.J.H. Wachters, Gaussian Basis Set for Molecular Wavefunctions Containing Third- Row Atoms, J. Chem. Phys. 52 (1970) 1033–1036. doi:10.1063/1.1673095.

[46] P.C. Hariharan, J.A. Pople, The influence of polarization functions on molecular orbital hydrogenation energies, Theor. Chim. Acta. 28 (1973) 213–222. doi:10.1007/BF00533485.

[47] C.A. Guido, E. Brémond, C. Adamo, P. Cortona, Communication: One third: A new recipe for the PBE0 paradigm, J. Chem. Phys. 138 (2013) 021104. doi:10.1063/1.4775591.

[48] M. Munzarova, M. Kaupp, A critical validation of density functional and coupled-cluster approaches for the calculation of EPR hyperfine coupling constants in transition metal complexes, J. Phys. Chem. A. 103 (1999) 9966–9983. doi:10.1021/jp992303p.

[49] W. Kutzelnigg, U. Fleischer, M. Schindler, The IGLO-Method: Ab-initio Calculation and Interpretation of NMR Chemical Shifts and Magnetic Susceptibilities, in: NMR Basic Princ. Prog., Springer-Verlag, Berlin, 1990: pp. 165–262. doi:10.1007/978-3-642-75932-1_3.

[50] F. Neese, The ORCA program system, Wiley Interdiscip. Rev. Comput. Mol. Sci. 2 (2012) 73–78. doi:10.1002/wcms.81.

[51] L. Noodleman, Valence bond description of antiferromagnetic coupling in transition metal dimers, J. Chem. Phys. 74 (1981) 5737. doi:10.1063/1.440939.

[52] J.G. Norman, P.B. Ryan, L. Noodleman, Electronic structure of 2-Fe ferredoxin models by X.alpha. valence bond theory, J. Am. Chem. Soc. 102 (1980) 4279–4282. doi:10.1021/ja00532a060.

[53] F. Neese, Calculation of the zero-field splitting tensor on the basis of hybrid density functional and Hartree-Fock theory, J. Chem. Phys. 127 (2007) 164112. doi:10.1063/1.2772857.

[54] Z. Ke, L.E. Jamieson, D.M. Dawson, S.E. Ashbrook, M. Bühl, NMR chemical shifts of urea loaded copper benzoate. A joint solid-state NMR and DFT study (Dataset)., University of St Andrews Research Portal. (2019). doi: https://doi.org/XXXX.